การประชุมวิชาการเครือข่ายวิศวกรรมเครื่องกลแห่งประเทศไทยครั้งที่ 14
2-3 พฤศจิกายน 2543 โรงแรม โนโวเทล เชียงใหม่

A Numerical and Experimental Investigation of the modeling of microwave drying using a rectangular wave guide

Phadungsak RATANADECHO, K. AOKI and M. AKAHORI
Nagaoka University of Technology, 1603-1, Kamitomioka, Nagaoka , Niigata, Japan , 940-2188
Email: phadu@blue.nagaokaut.ac.jp

Abstract

A detailed of mathematical model is presented, which uses a comprehensive two-dimensional heat and mass transport equations to describe the drying process, couple with a complete solution of the unsteady Maxwell's equations in the time domain, can be used to investigate numerous aspects of microwave drying of capillary porous packed bed using a rectangular wave guide. Most importantly, it focuses on the prediction of the distribution of electric field, temperature distribution and moisture distribution within the capillary porous medium. A comparison between numerical and experimental results for the microwave drying of capillary porous packed bed using rectangular wave guide is presented.

Key Words: Microwave Drying, Rectangular Wave Guide, Reflection, Capillary Porous Packed bed.

1. Introduction

A practical way to distinguish between the various drying process is to classify them by heating mode: convective drying, external radiative drying, vacuum drying and conductive drying. Drying with internal heat generation, such as dielectric drying or microwave drying, is a special case. Generally, microwave process exploits the polarization of molecules bonds, especially of polar water molecules, causing these bonds to vibrate, leading to a power dissipated as heat generation within the dielectric material. More recently, microwave technology can provide numerous advantages over conventional mechanical method. Some of these advantages include reduce the cost of system maintenance, provide more rapid and uniform heating, and offering improvements in product quality. In the past decade, microwave technology has been applied to many processes. Generally, the application of microwave heating is largely divided into two types, oven type and wave guide type. The oven type is very popular as a microwave oven but the great number of reflections occurs in an oven and the handling of the electromagnetic in the system is very difficult. This phenomenon explains why the rectangular wave guide type is used for this work. A number of analyses of conventional drying process and application of microwave process have appeared in the recent literature [1]-[3]. Also, this work, a comprehensive two-dimensional heat and mass transport equations to describe the drying process, couple with a complete solution of the unsteady Maxwell's equations in the time domain is presented.

2. Experimental Apparatus

Figure 1 shows the experimental apparatus for the drying system. The system was a monochromatic wave of $1E_{10}$ mode and operating at frequency 2.45GHz transmits along the z-direction of the rectangular wave guide with inner dimensions of 109.22×54.61 mm toward a water load that is situated at the end of the wave guide. The water load (lower absorbing boundary) ensures that only a minimal amount of microwave is reflected back to the sample, while a upper absorbing boundary, which is located at the front end of wave guide, is used to trap any microwave reflected from the sample damaging the magnetron. The sample (capillary porous packed bed) for studied is an initially partially saturated rectangular packed bed, which composes of glass beads and water with thickness of 50 mm, it is inserted in the rectangular wave guide. A container is made of polypropylene of 0.75 mm in thickness. The sample preparing and the measurement of porosity and permeability. For the dielectric properties at various conditions were measured [6]. During the experiment, the weight of the sample, the ambient temperature, the temperature of the sample at eight locations, the transmitted microwave power, the reflected microwave power, and the microwave power absorbed by the sample were recorded by a data logger that was connected to a computer.

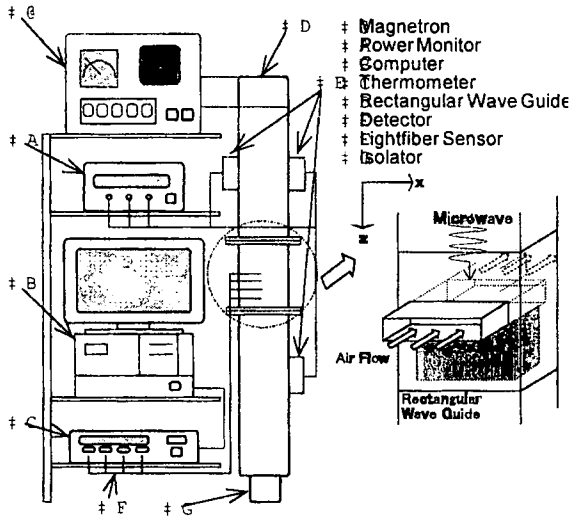

(a) Equipment list

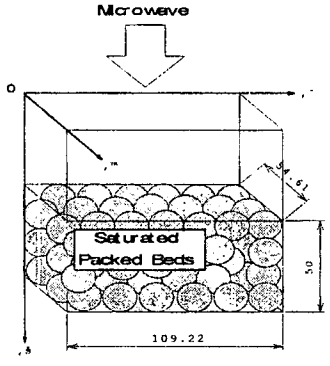

(b) rectangular porous packed bed

Fig.1 Experimental apparatus.

3. ANALYSIS OF MICROWAVE HEATING USING RECTANGULAR WAVE GUIDE

Generally, studies on the microwave drying involve solutions of the equations governing electromagnetic propagation, i.e. Maxwell's equations, either by themselves or coupled with the heat and mass transport equations. A two-dimensional analytical model over the x-z plane in Fig.2 is presented. The face of the sample is exposed to the external drying conditions. Microwave in the form of plane wave incident this surface. Another surfaces rests on impermeable and adiabatic surface. With this configuration it is possible that standing wave patterns can be generated within the sample.

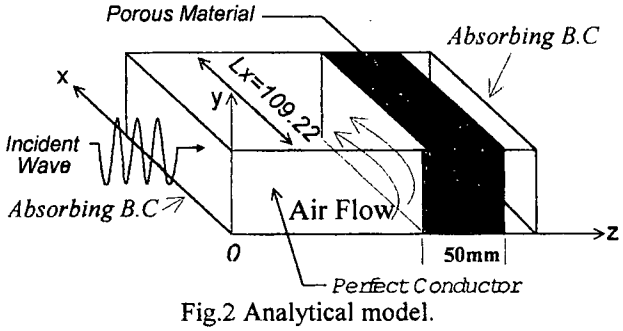

Fig.2 Analytical model.

3.1 Analysis of electromagnetic field

Assumptions. We consider analytical model showing the process of microwave heating for multi-layered materials. Figure 1 shows the analytical model for microwave heating using a rectangular wave guide. The model proposed is based on the following assumptions:

1. Since microwave of TE_{10} mode which propagates in rectangular wave guide is independent in y-direction, the electromagnetic field can be dealt with two-dimensional model on x-z plane.
2. The absorption of microwave for the cavity (including air) in a rectangular wave guide is negligible.
3. The walls of a rectangular wave guide are perfect conductors.
4. The effect of the sample container on electromagnetic field can be neglected.

Basic equations. The basic equations for the electromagnetic field are expressed as the Maxwell's relations. When microwave propagates though isotropic medium having permittivity ε, magnetic permeability μ, electric conductivity σ, and electric charge density q, the equations are given as follows;.

$$\nabla \times \boldsymbol{E} = -\frac{\partial \boldsymbol{B}}{\partial t} \tag{1}$$

$$\nabla \times \boldsymbol{H} = \boldsymbol{J} + \frac{\partial \boldsymbol{D}}{\partial t} \tag{2}$$

$$\nabla \cdot \boldsymbol{D} = q \tag{3}$$

$$\nabla \cdot \boldsymbol{B} = 0 \tag{4}$$

$\boldsymbol{E}$ is the electric field intensity, $\boldsymbol{H}$ is the magnetic field intensity, $\boldsymbol{J}$ is the current flux, $\boldsymbol{D}$ is the dielectric flux density, and $\boldsymbol{B}$ is the magnetic flux density. The relationships between these variables and electromagnetic properties are given by

$$\boldsymbol{D} = \varepsilon \boldsymbol{E} \tag{5}$$

$$\boldsymbol{B} = \mu \boldsymbol{H} \tag{6}$$

$$\boldsymbol{J} = \sigma \boldsymbol{E} \tag{7}$$

Substituting Eqs.(5)-(7) into Eqs.(1)-(4) yields the following equations which are represented by the only electric and magnetic field intensities.

$$\nabla \times \boldsymbol{E} = -\mu \frac{\partial \boldsymbol{H}}{\partial t} \tag{8}$$

$$\nabla \times \boldsymbol{H} = \sigma \boldsymbol{E} + \varepsilon \frac{\partial \boldsymbol{E}}{\partial t} \tag{9}$$

$$\nabla \cdot \boldsymbol{E} = \frac{q}{\varepsilon} \tag{10}$$

$$\nabla \cdot \boldsymbol{H} = 0 \tag{11}$$

For the microwave of TE_{10} mode, the components of electric and magnetic field intensities are given by

$$E_x = E_z = H_y = 0$$
$$E_y,\ H_x,\ H_z \neq 0 \tag{12}$$

where subscripts x, y and z represent x, y and z components of vectors, respectively. Taking into account the relation of Eq.(12), Eqs.(8)-(11) are written as, using the component notations of electric and magnetic field intensities,

$$\frac{\partial E_y}{\partial z} = \mu \frac{\partial H_x}{\partial t} \tag{13}$$

$$\frac{\partial E_y}{\partial x} = -\mu \frac{\partial H_z}{\partial t} \tag{14}$$

$$-\left(\frac{\partial H_z}{\partial x} - \frac{\partial H_x}{\partial z}\right) = \sigma E_y + \varepsilon \frac{\partial E_y}{\partial t} \tag{15}$$

where, permittivity ε, magnetic permeability μ and electric conductivity σ are given by

$$\varepsilon = \varepsilon_0 \varepsilon_r \tag{16}$$

$$\mu = \mu_0 \mu_r \tag{17}$$

$$\sigma = 2\pi f \varepsilon \tan\delta \tag{18}$$

where f is frequency of microwave, $\tan\delta$ is dielectric loss coefficient, ε_r and μ_r are relative permittivity and relative magnetic permeability, respectively. Further, because the dielectric properties are assumed to vary with temperature and moisture content during drying process and can taken the principle directly from the literature [8] .

Boundary conditions. Corresponding to the analytical model shown in Figure 1, boundary conditions can be given as follows:

(a) Perfectly conducting boundary condition

Boundary conditions on the inner wall surface of a rectangular wave guide are given as, using Faraday's law and Gauss' theorem

$$E_t = 0, \quad H_n = 0 \tag{19}$$

where subscripts t and n denote the components of tangential and normal directions, respectively.

(b) Continuity boundary condition

Boundary conditions on the interface between different materials, for example between air and dielectric material surface, are given as, using Ampere's law and Gauss' theorem

$$E_t = E'_t, \quad H_t = H'_t$$
$$D_n = D'_n, \quad B_n = B'_n \tag{20}$$

where superscript ' denotes one of different materials.

(c) Absorbing boundary condition

At both ends of rectangular wave guide, the first order absorbing conditions proposed by G. Mur [5] are applied.

$$\frac{\partial E_y}{\partial t} = \pm \upsilon \frac{\partial E_y}{\partial z} \tag{21}$$

Here, the symbol ± represent forward or backward waves and υ is phase velocity of microwave.

(d) Oscillation of the electric and magnetic flied intensities by magnetron

Incident wave due to magnetron is given by the following equations.

$$E_y = E_{yin} \sin\left(\frac{\pi x}{L_x}\right) \sin(2\pi f t) \tag{22}$$

$$H_x = \frac{E_{yin}}{Z_H} \sin\left(\frac{\pi x}{L_x}\right) \sin(2\pi f t) \tag{23}$$

E_{yin} is the input value of electric field intensity, L_x is the length of rectangular wave guide in x-direction, Z_H is the wave impedance in cases where microwave propagates in rectangular wave guide, and can be represented by

$$Z_H = \frac{\lambda_g Z_I}{\lambda} = \frac{\lambda_g}{\lambda} \sqrt{\frac{\mu}{\varepsilon}} \tag{24}$$

where Z_I depends on material and is called intrinsic impedance. Also, λ and λ_g are wave length of microwaves in free space and rectangular wave guide, respectively.

For the power flux associated with a propagating electromagnetic waves is represented by the Poynting vector S and time average flux for harmonic fields is defined as:

$$S = \frac{1}{2} \mathrm{Re}(E \times H^*) \tag{25}$$

where Re is real part

The poynting theorem allows the evaluation of the microwave power input. It is expressed as:

$$P_{in} = \int_A S.dA = \frac{A}{4z} E^2_{yin} \tag{26}$$

3.2 Analysis of heat and mass transport

A transient two-dimensional formulation is now described for fundamental studies of coupled heat and mass transport in the sample during the microwave drying using rectangular wave guide. Due to the complexity of the phenomena, and difficulty of finding actual situations in which the main assumptions involve in the formulation are:

1. Each of three phases of solid, liquid, and gas is continuous.
2. Local thermodynamics equilibrium is valid, which mean that the temperature in all phase is equal.
3. Simultaneous heat and mass transport at constant gaseous pressure, where the dominant mechanisms are capillary effects, vapor diffusion and gravity. Such is generally the case in the drying process of capillary porous medium at atmospheric pressure when the temperature is lower than the water boiling point.
4. The contribution of convection to energy transport is added.
5. Corresponding to electromagnetic field, temperature and moisture profiles also can be dealt with two-dimensional model on x-z plane.
6. The effect of the sample container on temperature and moisture profiles can be neglected.

Mass conservation

The macroscopic mass conservation for liquid, water vapor, air, and gas phase, are written, respectively, as

Liquid phase

$$\rho_l \phi \frac{\partial s}{\partial t} + \rho_l \frac{\partial u_l}{\partial x} + \rho_l \frac{\partial w_l}{\partial z} = -n \tag{27}$$

Vapor phase

$$\frac{\partial}{\partial t}\{\rho_v \phi(1-s)\} + \frac{\partial}{\partial x}[\rho_v u_v] + \frac{\partial}{\partial z}[\rho_v w_v] = n \tag{28}$$

Air phase

$$\frac{\partial}{\partial t}\{\rho_a \phi(1-s)\} + \frac{\partial}{\partial x}[\rho_a u_a] + \frac{\partial}{\partial z}[\rho_a w_a] = 0 \tag{29}$$

Gas phase

$$\frac{\partial}{\partial t}\{\rho_g \phi(1-s)\} + \frac{\partial}{\partial x}[\rho_g u_g] + \frac{\partial}{\partial z}[\rho_g w_g] = n \tag{30}$$

In which n is the evaporation rate during phase change, ϕ is the porosity of porous medium.

Energy conservation

The governing energy equation describing the temperature rise in the sample is the time dependent equation is

$$\frac{\partial}{\partial t}\left[\left(\rho c_p\right)_T T\right]+\nabla\left[\left\{\rho_l c_{pl} u_l+\left(\rho_a c_{pa}+\rho_v c_{pv}\right)u_g\right\}T\right]+H_v\overset{n}{} \quad (31)$$
$$=-\nabla q+Q$$

where Hv is the latent heat of vaporization of water and Q is the local electromagnetic heat generation term, which is a function of the electric field distribution and defined as

$$Q=2\pi\cdot f\cdot\varepsilon_0\cdot\varepsilon_r(\tan\delta)E_y^2 \quad (32)$$

where ε_r denotes relative dielectric constant, ε_0 denotes the permittivity of free space and $\tan\delta$ denotes the loss tangent.

Phenomenological relations

In order to complete the system of equations, the expressions for the superficial average velocity of liquid phase and gas phase the generalized Darcy's law is used:

$$\vec{u}_l=-\frac{KK_{rl}}{\mu_l}\left[\nabla p_g-\nabla p_c-\rho_l\vec{g}\right] \quad (33)$$

$$\vec{u}_g=-\frac{KK_{rg}}{\mu_g}\left[\nabla p_g-\rho_g\vec{g}\right] \quad (34)$$

For the velocity of vapor water and air phase the generalized Fick's law on two component gases mixture we obtained:

$$\rho_v\vec{u}_v=\rho_v\vec{u}_g-\rho_g D_m\nabla\left(\frac{\rho_v}{\rho_g}\right) \quad (35)$$

$$\rho_a\vec{u}_a=\rho_a\vec{u}_g-\rho_g D_m\nabla\left(\frac{\rho_a}{\rho_g}\right) \quad (36)$$

where the capillary pressure p_c is related to the gas and liquid phases can be written by

$$p_c=p_g-p_l \quad (37)$$

and D_m is the effective molecular mass diffusion[7]

$$D_m=\frac{2\phi}{3-\phi}(1-s)D \quad (38)$$

where D is the binary mass diffusion in plain media.

The Fourier's law is used to write the heat flux density through the porous medium

$$q=-\lambda\nabla T \quad (39)$$

Equilibrium relations

The system of conservation equations obtained for multiphase transport mode requires constitutive equation for relative permeabilities K_r, capillary pressure p_c, capillary pressure functions (Leverett functions) J, and the effective thermal conductivity λ. A typical set of constitutive relationships for liquid and gas system given by:

$$k_{rl}=s_e^3 \quad (40)$$

$$k_{rg}=(1-s_e)^3 \quad (41)$$

where s_e is the effective water saturation considered the erreducible water saturation s_{ir} and defined by

$$s_e=\frac{s-s_{ir}}{1-s_{ir}} \quad (42)$$

The capillary pressure p_c is further assumed to be adequately represented by Leverett's well know $J(s_e)$ functions, the relationship between the capillary pressure and the water saturation is defined by using Leverett functions $J(s_e)$

$$p_c=p_g-p_l=\frac{\sigma}{\sqrt{K/\phi}}J(s_e) \quad (43)$$

in which σ is the gas-liquid interfacial tension, where $J(s_e)$ Kaviany[3] was correlated imbitition capillary pressure data obtained by Leverett with

$$J(s_e)=0.325(1/s_e-1)^{0.217} \quad (44)$$

The effective thermal conductivity for capillary porous medium λ is also function of water saturation, can be written as

$$\lambda=\frac{0.8}{1+3.78e^{-5.95s}} \quad (45)$$

State Equations

The gas phase is assumed to be an ideal mixture of perfect gas, so that species' density can be determined by the state equations, with the classical definitions for total density of the gas ρ_g and the mass average velocity of the gas:

$$\rho_a=\frac{P_a M_a}{R_o T}\ ,\ \rho_v=\frac{P_v M_v}{R_o T}$$
$$\rho_g=\rho_a+\rho_v$$
$$P_a=\rho_a R_a T\ ,\ P_v=\rho_v R_v T$$
$$P_g=P_a+P_v$$
$$\rho_g u_g=\rho_a u_a+\rho_v u_v \quad (46)$$

The partial pressure of the vapor was considered as a function of temperature and defined by

$$P_v=C_0+(C_1+(C_2+(C_3+(C_4+C_5T)T)T)T)T \quad (47)$$

where

$$C_0=610.8, C_1=43.87, C_2=1.47, C_3=0.025,$$
$$C_4=2.88e-4, C_5=2.71e-6$$

Moisture transport equation

The phenomena of moisture transport in the sample is described by the mass conservation equations for liquid phase (Eq.27) and the water vapor portion of the gas phase (Eq.28) since it is total water content that is interest, these equations in two-dimensional scalar forms can be added together to yield an equation for the total moisture content, in the form:

$$\phi\frac{\partial}{\partial t}\{\rho_l s+\rho_v(1-s)\}+\frac{\partial}{\partial x}[\rho_l u_l+\rho_v u_v] \\ +\frac{\partial}{\partial z}[\rho_l w_l+\rho_v w_v]=0 \quad (48)$$

by using Darcy's generalized law equation (Eqs.(33),(34)) and Fick's law (Eqs.(35),(36)), the moisture transport equation is thus written:

$$\phi\frac{\partial}{\partial t}\{\rho_l s+\rho_v(1-s)\}+ \\ \frac{\partial}{\partial x}\left[\rho_l\frac{KK_{rl}}{\mu_l}\left(\frac{\partial p_c}{\partial x}-\frac{\partial p_g}{\partial x}+\rho_l g_x\right)+\right. \\ \left.\rho_v\frac{KK_{rg}}{\mu_l}\left(-\frac{\partial p_g}{\partial x}+\rho_g g_x\right)-D_m\frac{\partial\rho_v}{\partial x}\right]+ \quad (49) \\ \frac{\partial}{\partial z}\left[\rho_l\frac{KK_{rl}}{\mu_l}\left(\frac{\partial p_c}{\partial z}-\frac{\partial p_g}{\partial z}+\rho_l g_z\right)+\right. \\ \left.\rho_v\frac{KK_{rg}}{\mu_l}\left(-\frac{\partial p_g}{\partial z}+\rho_g g_z\right)-D_m\frac{\partial\rho_v}{\partial z}\right]=0$$

In addition, it is assumed that the total gradient pressure ($p_g = const$) and gravitational effect in x-direction are negligible, Eq.(49) become:

$$\phi\frac{\partial}{\partial t}\{\rho_l s+\rho_v(1-s)\}+ \\ \frac{\partial}{\partial x}\left[\rho_l\frac{KK_{rl}}{\mu_l}\left(\frac{\partial p_c}{\partial x}\right)-D_m\frac{\partial\rho_v}{\partial x}\right]+ \quad (50) \\ \frac{\partial}{\partial z}\left[\rho_l\frac{KK_{rl}}{\mu_l}\left(\frac{\partial p_c}{\partial z}+\rho_l g_z\right)+\right. \\ \left.\rho_v\frac{KK_{rg}}{\mu_l}(\rho_g g_z)-D_m\frac{\partial\rho_v}{\partial z}\right]=0$$

Heat transport equation

For the more interesting of a nonisothermal flow we must add the temperature as a dependent variable and write an equation, which expresses the conservation of energy for the case of two-dimensional model. Thus, the equation (31) leads to:

$$\frac{\partial}{\partial t}\left[(\rho c_p)_T T\right]+\frac{\partial}{\partial x}\left[\{\rho_l c_{pl}u_l+(\rho_a c_{pa}+\rho_v c_{pv})u_g\}T\right]+ \\ \frac{\partial}{\partial z}\left[\{\rho_l c_{pl}w_l+(\rho_a c_{pa}+\rho_v c_{pv})w_g\}T\right]+H_v n \quad (51) \\ =\frac{\partial}{\partial x}\left[\lambda\frac{\partial T}{\partial x}\right]+\frac{\partial}{\partial z}\left[\lambda\frac{\partial T}{\partial z}\right]+Q$$

where;

$$(\rho c_p)_T=\rho_l c_{pl}\phi s+\{(\rho c_p)_a+(\rho c_p)_v\}\phi(1-s)+\rho_p c_{pp}(1-\phi) \quad (52)$$

$$n=\frac{\partial}{\partial t}\{\rho_v\phi(1-s)\}+\frac{\partial}{\partial x}\left[-D_m\frac{\partial\rho_v}{\partial x}\right]+ \\ \frac{\partial}{\partial z}\left[\rho_v\frac{KK_{rg}}{\mu_g}\rho_g g_z-D_m\frac{\partial\rho_v}{\partial z}\right] \quad (53)$$

Boundary and initial conditions

There are two types of boundary conditions for solution of the governing equations are formulated by assuming that convective and mass transfer occurs at the open and impermeable boundary. The boundary conditions proposed for the open boundary of the sample, for the exchange of energy at the open boundary can be described in the following form:

$$-\lambda\frac{\partial T}{\partial z}=h_c(T-T_\infty)+n H_v \quad (54)$$

where h_c is the local heat transfer coefficient

for the mass transfer at the open boundary is modeled by means of a local constant mass transfer coefficient, that is the local water vapor flux density is described as:

$$\rho_l w_l+\rho_v w_v=h_{ms}(\rho_{vs}-\rho_{v\infty}) \quad (55)$$

in which h_{ms} is the local mass transfer coefficient, ρ_{vs} is the density of water vapor at the open boundary and $\rho_{v\infty}$ is reference vapor density in the gas phase surrounding the open boundary. Considering the boundary conditions at the closed boundary (symmetry-impermeable) that no heat and mass exchange take place:

$$\frac{\partial T}{\partial x}=\frac{\partial T}{\partial z}=0 \quad (56)$$

$$\frac{\partial u}{\partial x}=\frac{\partial w}{\partial z}=0 \quad (57)$$

The initial conditions are given by uniform initial temperature and moisture.

Numerical procedure

In order to obtain the electromagnetic field, finite difference time domain (FDTD) method is applied [4]. Concerning the system of nonlinear partial differential equations (Eqs.(50)-(57)) must be solved a method of finite differences base on the notation of control volume as described by Patankar [7]. Since the propagating velocity of microwave is so fast compared with the rate of heat and mass transfer, different time steps of *dt*=4 [ps] and 1[s] are used corresponding to electromagnetic field, temperature and moisture profiles calculations, respectively. The step size of space is *dx*=*dz*=1[mm]. Some of the input data for electromagnetic and thermo physical properties and drying conditions are given in Table 1..

Table.1
The drying conditions used in the computations

Drying conditions	Value
Glass beads size ,d (mm)	0.15, 0.4
Initial saturation, So	0.99
Initial temperature, To (C)	12
Irreducible saturation, Sir	0.006
Porosity, ϕ	0.385, 0.371
Heat transfer coefficient, hc(W/m2K)	100
Mass transfer coefficient, hm(m/s)	0.1
Surrounding temperature, T_∞ (C)	12

4. Results and Discussion

The experimental results for the microwave drying using capillary porous packed bed (glass beads+water) were compared with mathematical model simulations both to verify the model predictions.

4.1 Simulation of electric field in a rectangular wave guide

For understand the phenomenon of electric fields inside the rectangular wave guide, the simulation analysis is required. In Fig.3-5, shows the electric field of TE_{10} mode at different time step along with the center axis x=54.61 of a rectangular wave guide, for the case of a rectangular wave guide is empty (which corresponds to that of air) and for the case of the sample is inserted in the rectangular wave guide, vertical axis represent the intensity of electric field E_y, which is normalized to the amplitude of input electromagnetic wave, E_{yin}. Figure 3 shows the standing wave of TE_{10} mode, for the case of a rectangular wave guide is empty. A standing wave is formed by superimposition of the forward wave propagated from the wave input region, z=0 and of the reflected wave from the lower absorbing boundary, z=200 mm. In Fig.4 corresponding to the case when the sample is inserted in the rectangular wave guide, since the incident wave passing through the cavity having low permittivity is directly irradiated to the sample having high permittivity, the major part of incident wave is reflected on the surface of sample and the standing waves forms in the cavity forward to the sample. Figure 4 shows the electric field distribution for the early stage of drying process, the electric field within the sample is extinguished. However, the electric field distribution for the end stage of drying process, in which case after a majority of the moisture level inside the sample is decreased, the effect of reflection rate on the surface of the sample is low which to increase the penetration depth of the electromagnetic energy within the sample.

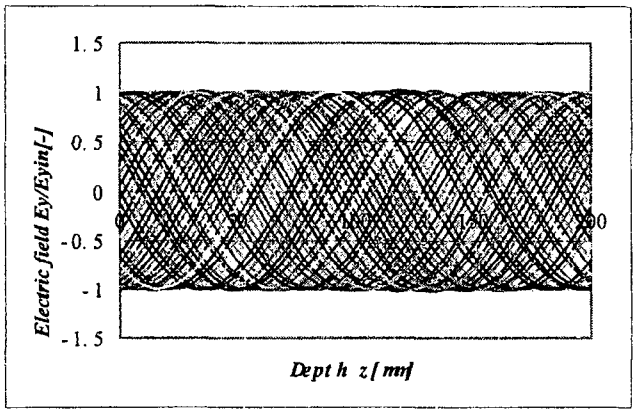

Fig.3. Distribution of electric field along the center axis for case of a rectangular wave guide is empty

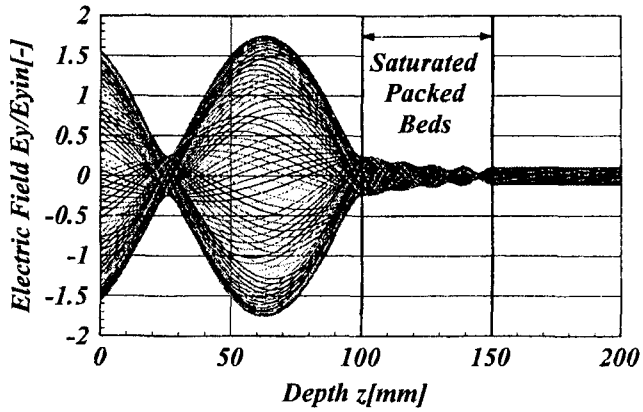

Fig.4. Distribution of electric field along the center axis for the sample is inserted in the rectangular wave guide (t=1 min)

4.2 The distribution of temperature and moisture profiles within the sample.

The mathematical model simulations results are compared with experimental drying data of microwave drying process are shows in Fig.5-12. The experimental and simulation of temperature profile as a function of distance at various times for the cases microwave power input of 100W are compared in Fig.5, which correspond to those of initial temperature with 12^{o}C, along with the center axis x=54.61 mm of rectangular wave guide. In contrast to that in conventional drying, the microwave drying is hotter inside drying sample and the surface temperature stay colder due to the cold of surrounding air, in the same time the evaporation take place at the surface of sample lower of temperature are experienced due to evaporative cooling. The simulated results were in agreement with the experimental results for the microwave drying process

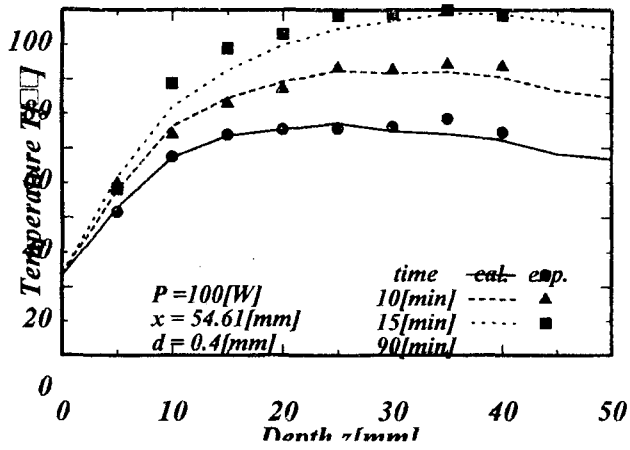

Fig.5. Temperature as a function of distance at various times (P=100w, d=0.4mm, x=54.61mm)

The experimental and simulation of temperature profile in times at various distances are compared in Figs.6. and 7. Figure 6 shows that the temperature profile within the sample rise up quickly in the early stage of drying process, after that it is slow down in the middle, In Fig.6, considering at the end stage of drying process, due to the moisture inside sample becomes reduce, decreasing the microwave power

absorbed, equilibrium is reached between microwave drying and convective losses by decreasing the temperature. However, at the higher microwave power input as shows in Fig.7, the temperature profile within the sample continuously rise up faster than case of lower microwave power input and the temperature remain high at the end stage of drying process. The simulated results were in agreement with the experimental results for the microwave drying process

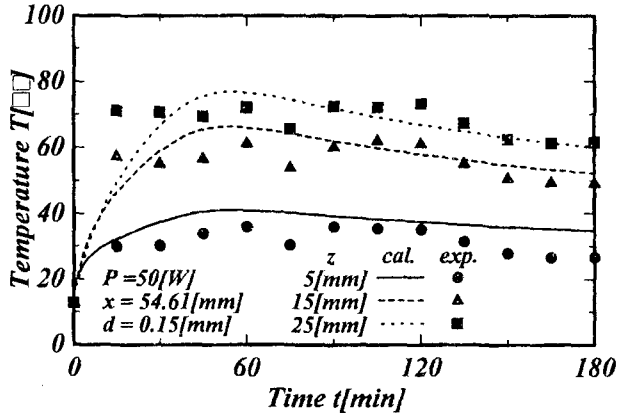

Fig.6. Temperature profile in times at various distances (P=50w, d=0.15mm, x=54.61mm)

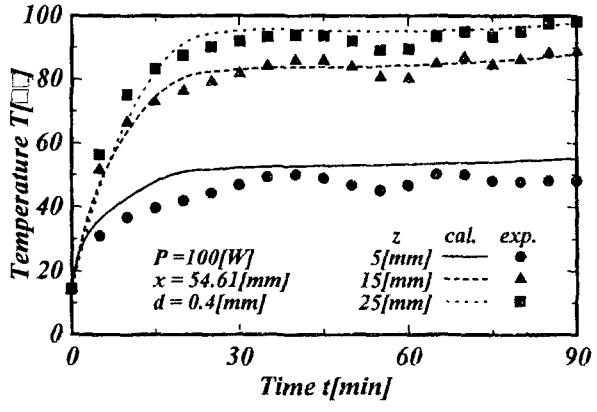

Fig.7. Temperature profile in times at various distances (P=100w, d=0.4mm, x=54.61mm)

Next discussion is a using different glass beads size at the same conditions. The temperature and moisture profile are shows in Fig.8, Fig.9 Fig.10, and Fig.11, respectively. Figures 8 and 9 shows the experimental results at the microwave power input of 100W and 50W, respectively, Fig.8 shows that the temperature profile on both cases (d=0.15mm and d=0.4mm) situated closet. However, the observed temperature profile at the leading edge of the sample in the case of small glass beads size are fundamentally higher than in the case of large glass beads size, this is because of the small glass beads size (which corresponds to a higher capillary force) can cause moisture to reach the surface in higher rate than case of large glass beads size (see Fig.10), correspond to an excess microwave power absorbed. Hence, even higher moisture content can lead to the higher temperature in this region. However, for the case of small glass beads size, the temperature profile deep inside the sample still lower due to the moisture inside sample becomes reduce. Continued drying process would eventually cause the average moisture content inside the sample would decrease and lead to decreased microwave power absorbed, reduced the temperature within the sample, especially, in the case of small glass beads size (Fig.10).

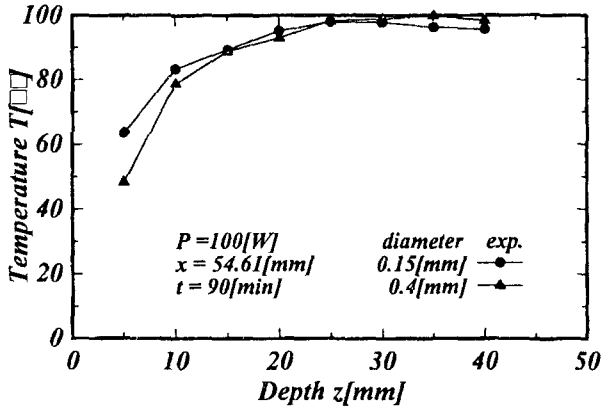

Fig.8. Comparison Temperature as a function of distance (P=100W t=90 min, x=54.61mm)

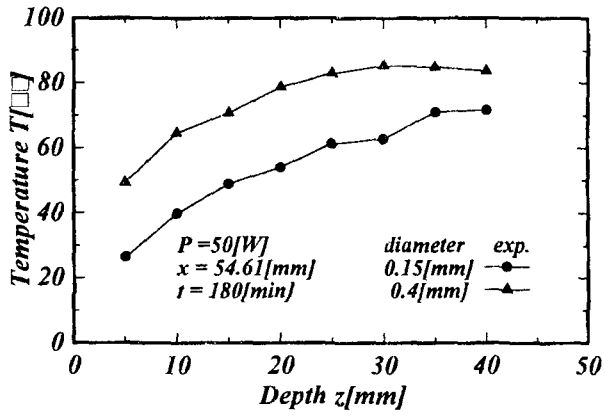

Fig.9. Comparison temperature as a function of distance (P=50W t=180 min, x=54.61mm)

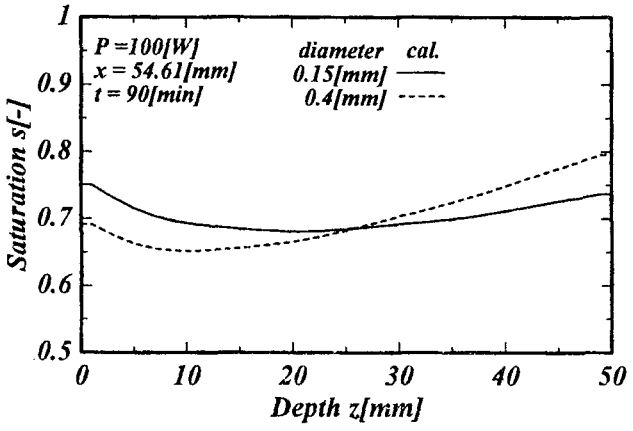

Fig.10. Comparison water saturation as a function of distance (P=100w t=90min, x=54.61mm)

The variation of drying rate with respect to time, both the simulation and experimental results are compared in Fig.11. The small glass beads size, however, leads to much higher capillary force results in a faster drying time and more uniform moisture profile inside the sample. The simulated results were in agreement with the experimental results for the microwave drying process.

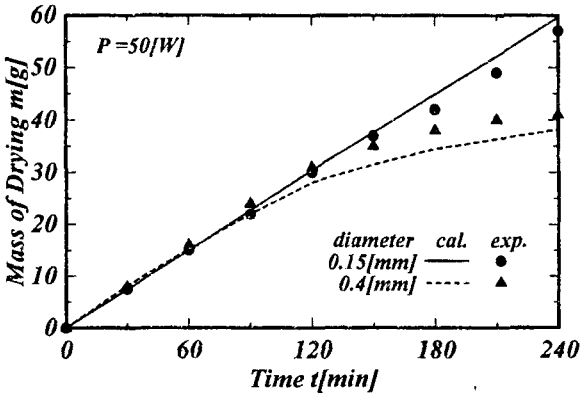

Fig.11. The variation of drying rate with respect to time (P=50W)

Figure 12 (a) shows the simulation of temperature distribution in the sample at time of 60s in the vertical plane (x-z), Figure 12(b) shows the experimental temperature distribution. It can be seen that the agreement between the two heating pattern is good, particularly concerning the location of the hot region. Most of the heating takes place on the inside of capillary porous packed beds, especially, at the middle region, and the surface temperature stay colder due to the cold of surrounding air, showing the capability of the mathematical model to correctly handle the field variations at the interfaces between materials of different dieletric properties

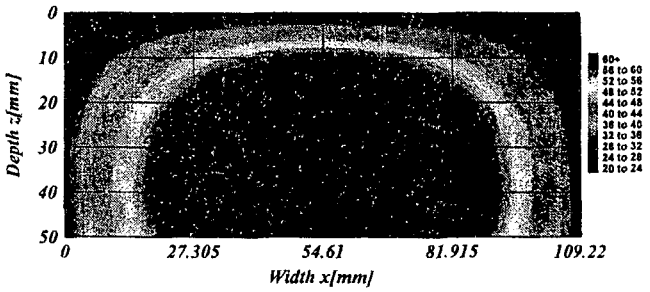

(a)

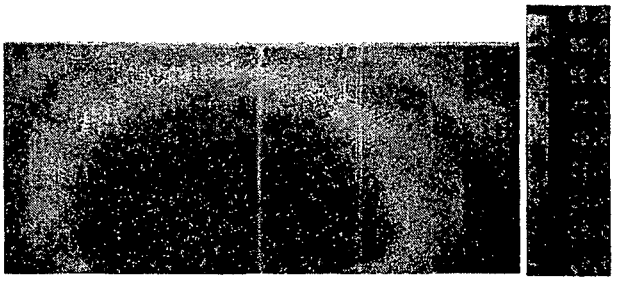

(b)

Fig. 12. Comparison between simulation results (a) and experimental results (b) for microwave drying of the sample using the microwave power input of 100W

5. Conclusions

The experiments and theoretically analysis of this study describe many of the predominate interactions within capillary porous medium during microwave drying using rectangular wave guide. The characteristics of microwave drying which are effected by the reflection of microwave and standing wave and depend on dielectric properties, moisture content, glass beads size and microwave power input, this work have been investigated numerically and experimentally. The following knowledge concerning the microwave drying phenomena is obtained:

1) The results of electromagnetic fields inside a rectangular wave guide and the sample shows that the varies of moisture content within the sample during microwave drying and the changing of glass bead size could enable change the location of the maximum intensity and distribution of electromagnetic field within the sample, this is because the dielectric properties strongly affects the electromagnetic field pattern and the behavior of the dielectric properties is influenced primarily by that of moisture content.

2) Nevertheless, the results of temperature and moisture profiles within the sample corresponds to the result of the electromagnetic fields, since the affect the microwave power absorbed, thus effect variation of the temperature and moisture profiles within the sample.

6. NOMENCLATURE

A	width of wave guide [m]
a	thermal diffusivity [m^2/s]
b	high of wave guide [m]
B	magnetic flux density [Wb/m^2]

C_p	specific heat capacity [J/kgK]
D	dielectric flux density [C/ m^2]
E	electric field intensity [V/m]
f	frequency of incident wave [Hz]
g	gravitational constant [m/s^2]
H	magnetic field intensity [A/m]
J	current flux [A/m^2]
L	length of a rectangular wave guide [m]
M	molecular weight [kg/kmol]
P	pressure [Pa]
Q	electromagnetic heat generation [W/m^3]
q	electric charge density [C/m^3]
R	universal gas constant [J/mol/K]
S	water saturation [-]
T	temperature [C]
t	time [s]
$\tan\delta$	loss tangent [-]
x, y, z	Cartesian coordinates [-]
Z_H	wave impedance [Ω]
Z_I	impedance [Ω]

Greek letters

ϕ	porosity [m^3 / m^3]
ρ	density [kg/m^3]
ε	permittivity [F/m]
ε_r	relative permittivity [F/m]
λ	free space wave length [m]
λ_g	wave guide wave length [m]
μ	permeability [H/m]
μ_o	free space permeability [H/m]
μ_r	relative permeability [H/m]
υ	velocity of propagation [m/s]
σ	electric conductivity [S/m]
ω	angular frequency [rad/s]

Subscripts

a	air
c	capillary
g	gas
j	layer number
n	normal component
p	particle
t	tangential component
w	water
x, y, z	coordinates

7. REFERENCES

1. A.C. Metaxas, R.J. Meridith, Industrial Microwave Heating, Peter Peregrinus, Ltd., London,1983.
2. C.K. Wei, H.T. Davis, E.A. Davis, J. Gordon, Heat and mass transfer in water-laden sand stone: microwave heating, A.I.Ch.E J. 31(5), 842-848 (1985).
3. M. Kaviany, Principle of Heat Transfer in Porous Media, Springer, Newyork, 1991.
4. K.S. Yee, Numerical solution of initial boundary value problems involving Maxwell's equation in isotropic media, IEEE Transcations of Antennas Progation AP-14 (1966) 302-307.
5. G. Mur, Absorbing Boundary conditions for the Finite-Difference Approximation of the Time-Domain Electromagnetic-Field Equations, IEEE Transcations of Electromagnetic Compatibility EMC-23 (4) (1981) 377-382.
6. A.R. Von Hippel, Dielectric Materials and Applications, MIT Press, Boston, 1954.
7. S.V. Patankar, Numerical Heat Transfer and Fluid Flow, Hemisphere Publishing Corporation, New York, 1980.
8. J. Wang, T. Schmugge, An Empirical model for the Complex Dielectric Permittivity of Soil as a Function of Water Content, IEEE Transactions on geoscience and remote sensing GE-18 (4) (1980) 288-295